Physica Scripta. Vol. 41, 304–315, 1990.

Group Theory and the Diffusion of Molecules, Dynamics and Structure

M. W. Evans* and D. M. Heyes

Department of Chemistry, Bourne Laboratory, Royal Holloway and Bedford New College, University of London, Egham, Surrey TW20 0EW, U.K.

Received August 18, 1988; in revised form June 15, 1989; accepted August 20, 1989

Abstract

Point group theory is used in the laboratory and molecule fixed frames (X, Y, Z) and (x, y, z) respectively to develop three principles upon which to base the analysis of diffusional processes in N particle atomic and molecular ensembles. The symmetry signatures of ensemble averages at field free equilibrium, and in the steady state under applied external fields are given in the point group $R_h(3)$ and in thirty-six molecular point groups. Physical examples of "group theoretical statistical mechanics" (g.t.s.m.) are given in terms of a new interpretation of the Weissenberg effect and of a theoretical prediction of shear induced depolarized light scattering. New fluctuation–dissipation theorems are developed from the principles and applications of g.t.s.m. for an applied electric field of arbitrary strength, and some corroborative computer simulations reported for liquid water and methyl chloride. Structural applications are discussed finally in the form of angularly resolved pair radial distribution functions.

Introduction

Developments in the computer simulation of molecular diffusional processes over the last decade [1–5] have emphasised the role of the molecule fixed frame (x, y, z) as well as that of the laboratory frame (X, Y, Z). Systematic computer simulation has emphasised a set of non-vanishing time correlation functions, some of which exist in frame (x, y, z) but vanish in frame (X, Y, Z) for all t. Conventional diffusion theory [6–8] usually focusses on frame (X, Y, Z), and in consequence may provide only a partially adequate picture of the molecular dynamical process. An example is the simple cross correlation function (c.c.f.) $\langle \boldsymbol{v}(0)\boldsymbol{\omega}(t)\rangle$ between a diffusing molecule's linear and angular velocities. This vanishes in frame (X, Y, Z) but exists in frame (x, y, z) for most molecular symmetries. The theory of rotational diffusion, and off-shoots such as the itinerant librator, neglect the existence of the c.c.f. in both frames of reference, and are therefore unable to describe the results of computer simulation [1–5] without fundamental modification.

Recently, the computer simulation results have been analysed systematically by Whiffen with point group theory [9] in both frames of reference, and detailed agreement was found with the computer simulation results on the C_{2v} molecule dichloromethane. This work has subsequently been developed into the three principles of group theoretical statistical mechanics (g.t.s.m.) [10–12] and applied to Couette flow [13–15] in which a strain rate of the type $\partial v_x/\partial Z$ is generated by the applied shear stress [16–18]. The application of g.t.s.m. in this context anticipated the existence of new c.c.f.'s in frame (X, Y, Z) which classical rheology leaves unconsidered. Subsequent computer simulation [16–18] revealed that these had the remarkable property of being asymmetric in the indices X and Z of the strain rate, as typified by the linear velocity c.c.f.

$$\langle v_X(0)v_Z(t)\rangle \neq \langle v_Z(0)v_X(t)\rangle \tag{1}$$

and this has been explained with g.t.s.m. [19] using a weighted combination of a shear induced antisymmetric c.c.f. of the type

$$\langle v_X(0)v_Z(t)\rangle = -\langle v_Z(0)v_X(t)\rangle \tag{2}$$

describing shear induced vorticity, and a symmetric component

$$\langle v_X(0)v_Z(t)\rangle = \langle v_Z(0)v_X(t)\rangle \tag{3}$$

describing shear induced deformation.

The result (1), observable in the computer simulation of atomic ensembles under applied shear [16–18], is a weighted combination of eqs. (2) and (3), which have the D symmetries (see later) $D_g^{(1)}$ and $D_g^{(2)}$ respectively.

The combined use of g.t.s.m. and non-equilibrium computer simulation [16–18] also showed the existence of new c.c.f.'s between components of the pressure tensor (or stress tensor), which provided a fundamental explanation for the well known Weissenberg effect of rheology [13–15], the pressure observed experimentally perpendicular to the plane of shear. These new c.c.f.'s have no counterparts in "classical" or customary rheology, in the same way that customary diffusion theory has no way of explaining many of the new c.c.f.'s discovered in diffusing molecules by computer simulation [1–5]. In deriving the new c.c.f.'s of type (1), and in explaining the Weissenberg effect, g.t.s.m. was able to guide the computer simulation, which in turn has been able to explain the well known experimental Weissenberg effect in terms of the dynamics of diffusing atoms.

In this paper the methods of g.t.s.m. are applied to molecular ensembles under the influence of external fields of various types, with the emphasis on shear. Non-equilibrium molecular dynamics (n.e.m.d.) has not yet advanced to the stage where molecular ensembles can be investigated with SLLOD and PUT algorithms [16–18] with the facility of atomic ensembles, where the method has rapidly become well established [20–25]. Molecular ensembles under shear differ fundamentally from their atomic counterparts, where the frame (x, y, z) is not defined, and a complete understanding of the effects of shear needs both frames. In the context of g.t.s.m. this leads to the consideration of a molecule fixed frame (x, y, z) defined conventionally in the literature point group character tables [26, 27], i.e. the symmetry elements are defined with respect to the (x, y, z) which appear in the standard character tables [26, 27] in the right hand side columns.

* Also at I.B.M., Data Systems Dividion, Neighborhood Road, Kingston, New York 12401, U.S.A.

Similarly, computer simulation and g.t.s.m. have shown the need for both frames when considering the effects of other types of fields, for example electric [28–30] and magnetic fields, and both frames are also needed at field-free equilibrium [1–5]. It is futile to argue in this context that observations can only be made in frame (X, Y, Z), because these observations are governed by processes which are visible statistically only in frame (x, y, z). If these latter are neglected, the interpretation we put on our observations is fallacious. The customary view can also overlook important details [16–18] in frame (X, Y, Z).

A correct understanding of processes in both frames is provided by g.t.s.m., which is used in this paper as a guide to future n.e.m.d. computer simulations of sheared molecular liquids; and to the various effects of applied electric and magnetic fields. Emphasis is put on the physical consequencies, using new fluctuation–dissipation theorems based on the new relation derived by Morriss and Evans [31], valid for arbitrary applied field strength, i.e. for linear and nonlinear response processes. The group theoretical details are presented mainly in tabular form, suitable for reference in several different contexts, so as not to overload the paper with mathematical detail. Familiarity with elementary group theory, as applied in chemical physics, is assumed from the outset.

The paper is arranged as follows. In Part 1 the three principles of g.t.s.m. are stated with reference to both frames. In Part 2, some basic symmetry concepts lead to Table I, in which the general symmetry of shear strain is given in frame (X, Y, Z), and for thirty six of the molecular point groups. Part 3 provides examples of application with emphasis on shear, the Weissenberg effect, and suggests in this context a new form of depolarised light scattering. There is also some discussion of the effects of electric and magnetic fields in both frames. Part 4 introduces new fluctuation-dissipation theorems based on the symmetry arguments of Part 2, and Part 5 finally deals with aspects of computer simulation, both conventional and non-equilibrium.

1. The principles of group theoretical statistical mechanics

These have been developed [19] from the Neumann Principle [32–34] and its extension by Whiffen [9] to the frame (x, y, z). They can be stated as follows.

Principle 1

The thermodynamic ensemble average $\langle \boldsymbol{ABCD} \ldots \rangle$ over the product $\boldsymbol{ABCD} \ldots$ exists in frame (X, Y, Z) if the product of representations $\Gamma(\boldsymbol{A})\Gamma(\boldsymbol{B})\Gamma(\boldsymbol{C}) \ldots$ contains the totally symmetric representation (t.s.r.) of the point group $R_h(3)$ of isotropic atomic or molecular ensembles.

Principle 2

This ensemble average exists in the molecule fixed frame (x, y, z) if the product of symmetry representations in the molecular point group contains that point group's t.s.r. at least once [9].

Principle 3

If an external field of force is applied to an atomic or molecular ensemble which subsequently reaches a steady state in the presence of that field, new ensemble averages may be created whose symmetry is that of the applied field.

In order to illustrate these Principles we provide a description of some symmetry properties of $R_h(3)$ in the following section.

2. Some symmetry concepts

The point group $R_h(3)$ is the symmetry group of isotropic three dimensional space. Its irreducible representations are $D_g^{(0)}, \ldots, D_g^{(n)}$ and $D_u^{(0)}, \ldots, D_u^{(n)}$ respectively. These are even (g) and odd (u) to the parity reversal $(X, Y, Z) \rightarrow (-X, -Y, -Z)$. A scalar in this notation has symmetry $D_g^{(0)}$, a pseudo-scalar is $D_u^{(0)}$, a polar vector such as $\boldsymbol{v}$ the centre of mass velocity, is $D_u^{(1)}$ and an axial vector such as angular velocity $(\boldsymbol{\omega})$ is $D_g^{(1)}$. The principles of Section 1 imply that in isotropic environments such as those of atomic or molecular ensembles, the symmetry of the ensemble average $\langle \boldsymbol{A} \rangle$ over the physical property $\boldsymbol{A}$ will be that of $\boldsymbol{A}$ itself, either in the laboratory or molecule fixed frames. The symmetry of the ensemble average $\langle \boldsymbol{AB} \rangle$ is given by the product of representations $\Gamma(\boldsymbol{A})\Gamma(\boldsymbol{B})$, where Γ denotes the symmetry representation in the point group of interest. The latter is $R_h(3)$ in frame (X, Y, Z) and the molecular point group in frame (x, y, z). Thus, the average $\langle \boldsymbol{AB} \rangle$ over the product of molecular physical properties $\boldsymbol{AB}$ exists in an isotropic molecular ensemble if $\Gamma(\boldsymbol{A})\Gamma(\boldsymbol{B})$ contains the totally symmetric representation (t.s.r.) at least once.

In $R_h(3)$ the t.s.r. is $D_g^{(0)}$, and ensemble averages over scalars exist in chiral media, and have opposite sign for each enantiomorph. Ensemble averages over both polar and axial vectors vanish at isotropic equilibrium because the symmetry representations of these quantities do not contain the t.s.r. These considerations can be extended to higher order tensors and also to products, such as time correlation functions. Thus, the generic auto correlation function $\langle \boldsymbol{A}(0) \cdot \boldsymbol{A}(t) \rangle$ exists in frame (X, Y, Z) because the product of representations

$$\Gamma(\boldsymbol{A})\Gamma(\boldsymbol{A}) = D_g^{(0)} + D_g^{(1)} + D_g^{(2)} \tag{4}$$

contains the t.s.r. once, representing the trace of the matrix product $\langle \boldsymbol{A}(0)\boldsymbol{A}(t) \rangle$. In eq. (4) we have used the Clebsch–Gordan Theorem

$$D^{(n)}D^{(m)} = D^{(n+m)} + \cdots + D^{|(n-m)|} \tag{5}$$

to expand the product the product of symmetry representations on the left-hand side. The expansion on the right hand side of this equation contains three terms, the scalar, vector and tensor products, respectively $D_g^{(0)}$, $D_g^{(1)}$, and $D_g^{(2)}$. The vector product of two vectors is another vector, and can be denoted

$$\text{Vector product part of } \langle \boldsymbol{A}(t)\boldsymbol{A}(0) \rangle = \langle \boldsymbol{A}(t) \times \boldsymbol{A}(0) \rangle$$

$$= \left\langle \begin{vmatrix} \boldsymbol{i} & \boldsymbol{j} & \boldsymbol{k} \\ A_X(t) & A_Y(t) & A_Z(t) \\ A_X(0) & A_Y(0) & A_Z(0) \end{vmatrix} \right\rangle \tag{6}$$

The overal symmetry of this vector is $D_g^{(1)}$. Here $\boldsymbol{i}, \boldsymbol{j}$, and $\boldsymbol{k}$ are unit vectors in the axes X, Y, and Z respectively. If we

Table I. Symmetry data for thirty-six molecular point groups.

Point Group	Scalar ($D_g^{(0)}$)	Scalar ($D_g^{(0)}$)	Vector ($D_g^{(1)}$)	Vector ($D_u^{(1)}$)	$D_g^{(1)}D_g^{(1)} = D_u^{(1)}D_u^{(1)} = D_g^{(0)} + D_g^{(1)} + D_g^{(2)}$	$D_u^{(1)}D_g^{(1)} = D_u^{(0)} + D_u^{(1)} + D_u^{(2)}$	No.	No.	Local symmetry
C_1 (1)	A	A	$3A$	$3A$	$9A$	$9A$	9	9	triclinic
$C_i(S_2)$ ($\bar{1}$)	A_g	A_g	$3A_g$	$3A_u$	$9A_g$	$9A_u$	9	0	triclinic
C_2 (2)	A	A	$A + 2B$	$A + 2B$	$5A + 4B$	$5A + 4B$	5	5	monoclinic
C_{1h} (m)	A'	A''	$A' + 2A''$	$2A' + A''$	$5A' + 4A''$	$4A' + 5A''$	5	4	monoclinic
C_{2h}(2/m)	A_g	A_u	$A_g + 2B_g$	$A_u + 2B_u$	$5A_g + 4B_g$	$5A_u + 4B_u$	5	0	monoclinic
C_{2v} (2mm)	A_1	A_2	$A_2 + B_1 + B_2$	$A_1 + B_1 + B_2$	$3A_1 + 2B_1 + 2B_2 + 2A_2$	$2A_1 + 3A_2 + 2B_1 + 2B_2$	3	2	orthorhombic
D_2 (232)	A_1	A_1	$B_1 + B_2 + B_3$	$B_1 + B_2 + B_3$	$3A_1 + 2B_1 + 2B_2 + 2B_3$	$3A_1 + 2B_1 + 2B_2 + 2B_3$	3	3	orthorhombic
D_{2h} (mmm)	A_{1g}	A_{1u}	$B_{1g} + B_{2g} + B_{3g}$	$B_{1u} + B_{2u} + B_{3u}$	$3A_{1g} + 2B_{1g} + 2B_{2g} + 2B_{3g}$	$3A_{1u} + 2B_{1u} + 2B_{2u} + 2B_{3u}$	3	0	orthorhombic
C_3 (3)	A	A	$A + E$	$A + E$	$3A + 3E$	$3A + 3E$	2	2	trigonal
C_{3v} (3m)	A_1	A_2	$A_2 + E$	$A_1 + E$	$2A_1 + A_2 + 3E$	$A_1 + 2A_2 + 3E$	2	1	trigonal
D_3 (32)	A_1	A_1	$A_2 + E$	$A_2 + E$	$2A_1 + A_2 + 3E$	$2A_1 + A_2 + 3E$	2	2	trigonal
D_{3d} ($\bar{3}m$)	A_{1g}	A_{1u}	$A_{2g} + E_g$	$A_{2u} + E_u$	$2A_{1g} + A_{2g} + 3E_g$	$2A_{1u} + A_{2u} + 3E_u$	2	0	trigonal
S_6 ($\bar{3}$)	A_g	A_u	$A_g + E_g$	$A_u + E_u$	$3A_g + 3E_g$	$3A_u + 3E_u$	3	0	trigonal
C_4 (4)	A	A	$A + E$	$A + E$	$3A + 2B + \mathrm{E}$	$3A + 2B + 2E$	3	3	tetragonal
C_{4v} (4mm)	A_1	A_2	$A_2 + E$	$A_1 + E$	$2A_1 + A_2 + B_1 + B_2 + 2E$	$A_1 + 2A_2 + B_1 + B_2 + 2E$	2	1	tetragonal
C_{4h} (4/m)	A_g	A_u	$A_g + E_g$	$A_u + E_u$	$3A_g + 2B_g + 2E_g$	$3A_u + 2B_u + 2E_u$	2	0	tetragonal
D_4 (422)	A_1	A_1	$A_2 + E$	$A_2 + E$	$2A_1 + A_2 + B_1 + B_2 + 2E$	$2A_1 + A_2 + B_1 + B_2 + 2E$	2	2	tetragonal
D_{4h} (4/mmm)	A_{1g}	A_{1u}	$A_{2g} + E_g$	$A_{2u} + E_u$	$2A_{1g} + A_{2g} + B_{1g} + B_{2g} + 2E_g$	$2A_{1u} + A_{2u} + B_{1u} + B_{2u} + 2E_u$	2	0	tetragonal
D_{2d} ($\bar{4}2m$)	A_1	B_1	$A_2 + E$	$B_2 + E$	$2A_1 + A_2 + B_1 + B_2 + 2E$	$A_1 + A_2 + 2B_1 + B_2 + 2E$	2	1	tetragonal
S_4 ($\bar{4}$)	A	B	$A + E$	$B + E$	$3A + 2B + 2E$	$2A + 3B + 2E$	3	2	tetragonal
C_6 (6)	A	A	$A + E_1$	$A + E_1$	$3A + 2E_1 + E_2$	$3A + 2E_1 + E_2$	3	3	hexagonal
C_{6v} (6mm)	A_1	A_2	$A_2 + E_1$	$A_1 + E_1$	$2A_1 + A_2 + 2E_1 + E_2$	$A_1 + A_2 + 2E_1 + E_2$	2	1	hexagonal
C_{3h} ($\bar{6}$)	A'	A''	$A' + E''$	$A'' + E'$	$3A' + 2E'' + E'$	$3A'' + 3E''$	3	0	hexagonal
C_{6h} (6/m)	A_g	A_u	$A_g + E_{1g}$	$A_u + E_{1u}$	$3A_g + 2E_{1g} + E_{2g}$	$3A_u + 2E_{1u} + E_{2u}$	3	0	hexagonal
D_6 (622)	A_1	A_1	$A_2 + E_1$	$A_2 + E_1$	$2A_1 + A_2 + E_2 + 2E_1$	$2A_1 + A_2 + E_2 + 2E_1$	2	2	hexagonal
D_{3h} (6m2)	A_1'	A_1''	$A_2' + E''$	$A_2'' + E'$	$2A_1' + A_2' + E' + 2E''$	$2A_1'' + A_2'' + 2E' + E''$	2	0	hexagonal
D_{6h} (6/mmm)	A_{1g}	A_{1u}	$A_{2g} + E_{1g}$	$A_{2u} + E_{1u}$	$2A_{1g} + A_{2g} + 2E_{1g} + E_{2g}$	$2A_{1u} + A_{2u} + 2E_{1u} + E_{2u}$	2	0	hexagonal
T_d ($\bar{4}3m$)	A_1	A_2	T_1	T_2	$A_1 + T_1 + E + T_2$	$A_2 + T_2 + E + T_1$	1	0	cubic
O_h ($m3m$)	A_{1g}	A_{1u}	T_{1g}	T_{1u}	$A_{1g} + T_{1g} + E_g + T_{2g}$	$A_{1u} + T_{1u} + E_u + T_{2u}$	1	0	cubic
T (23)	A	A	T	T	$A + E + 2T$	$A + E + 2T$	1	1	cubic
T_h ($m3$)	A_g	A_u	T_g	T_u	$A_g + E_g + 2T_g$	$A_u + E_u + 2T_u$	1	0	cubic
O (434)	A_1	A_1	T_1	T_1	$A_1 + E + T_1 + T_2$	$A_1 + E + T_1 + T_2$	1	1	cubic
$C_{\infty v}$	Σ^+	Σ^-	$\Sigma^- + \Pi$	$\Sigma^+ + \Pi$	$2\Sigma^+ + \Sigma^- + 2\Pi + \Delta$	$2\Sigma^- + \Sigma^+ + 2\Pi + \Delta$	2	1	linear dipolar
C_∞	Σ	Σ	$\Sigma + \Pi$	$\Sigma + \Pi$	$3\Sigma + 2\Pi + \Delta$	$3\Sigma + 2\Pi + \Delta$	3	3	linear diplar chiral
$D_{\infty h}$	Σ_g^+	Σ_u^-	$\Sigma_g^- + \Pi_g$	$\Sigma_u^+ + \Pi_u$	$2\Sigma_g^+ + \Sigma_g^- + 2\Pi_g + \Delta_g$	$2\Sigma_u^- + \Sigma_u^+ + 2\Pi_u + \Delta_u$	2	0	linear non-dipolar
D_∞	Σ^+	Σ^+	$\Sigma^- + \Pi$	$\Sigma^- + \Pi$	$2\Sigma^+ + \Sigma^- + 2\Pi + \Delta$	$2\Sigma^- + \Sigma^+ + 2\Pi + \Delta$	2	2	linear non-dipolar chiral

examine an individual component of the determinant on the right hand side of eq. (6), for example the $\boldsymbol{j}$ component, we find

$$\{\langle \boldsymbol{A}(t) \times \boldsymbol{A}(0)\rangle\}_j = \{\langle A_Z(t)A_X(0)\rangle - \langle A_X(t)A_Z(0)\rangle\}\boldsymbol{j} \tag{7}$$

with similar results for the other components.

The overall symmetry is however $D_g^{(1)}$, and does not contain the t.s.r. By Principle 1 these averages all vanish, therefore, at field-free (isotropic) equilibrium, but by Principle 3, may exist in frame (X, Y, Z) in the presence of an external field of the correct symmetry.

Similarly, the tensor product of two vectors is a tensor, a three by three matrix, the dyadic product

$$\text{tensor part of } \langle \boldsymbol{A}(t)\boldsymbol{A}(0)\rangle = \left\langle \begin{bmatrix} A_X(t)A_X(0)\boldsymbol{ii}^T & A_X(t)A_Y(0)\boldsymbol{ji}^T & A_X(t)A_Z(0)\boldsymbol{ki}^T \\ A_Y(t)A_X(0)\boldsymbol{ij}^T & A_Y(t)A_Y(0)\boldsymbol{jj}^T & A_Y(t)A_Z(0)\boldsymbol{kj}^T \\ A_Z(t)A_X(0)\boldsymbol{ik}^T & A_Z(t)A_Y(0)\boldsymbol{jk}^T & A_Z(t)A_Y(0)\boldsymbol{kk}^T \end{bmatrix} \right\rangle \tag{8}$$

where

$$\boldsymbol{ij}^T = \begin{bmatrix} 0 & 1 & 0 \\ 0 & 0 & 0 \\ 0 & 0 & 0 \end{bmatrix} \tag{9}$$

and so on. The overall symmetry in eq. (8) is the symmetric second rank $D_g^{(2)}$ and does not contain the t.s.r. so that these ensemble averages all vanish at field-free equilibrium. The matrix is symmetric (D rank 2) so that there is index symmetry in the off-diagonal elements, giving results such as eq. (3).

2.1. *The effect of fields, Principle 3*

An applied field of force has its own symmetry signature in a given point group, and in frame (X, Y, Z) this is a D representation. By Principle 3 ensemble averages with the same representation may appear in the N particle ensemble at the field-on steady state. An electric field, $\boldsymbol{E}$, for example, is a polar vector of $D_u^{(1)}$ symmetry; a magnetic field $\boldsymbol{B}$ is an axial vector of $D_g^{(1)}$ symmetry, and a shearing rate of the type $\partial v_X/\partial Z$ has the symmetry [16–18] $D_g^{(0)} + D_g^{(1)} + D_g^{(2)}$.

In addition to the ensemble averages that may exist at field-free equilibrium, applied fields set up new ensemble averages in frame (X, Y, Z) whose symmetry, by Principle 3, is that of the field. For example, an electric field sets up averages of the type $\langle \boldsymbol{\omega}(t) \times \boldsymbol{v}(0)\rangle$ similar to those of eq. (6), but whose symmetry is $D_u^{(1)}$. These have been detected by computer simulation [20–25] in the form of component ensemble averages which have the property

$$E_Y \text{ induces } \langle \omega_X(t)v_Z(0)\rangle = -\langle \omega_Z(t)v_X(0)\rangle \tag{10}$$

and similarly for the X and Z components of the applied field. These are antisymmetric time c.c.f.'s which vanish at field free equilibrium, and have overall symmetry $D_u^{(1)}$. They were found by computer simulation and are not considered in the conventional theory of diffusion.

Similarly, the response of an ensemble of atoms to shear is described by a combination of $D_g^{(1)}$ (vector) symmetry of Type 6 or 7, and a tensor symmetry $D_g^{(2)}$ of Type 8. For a strain rate $\partial v_X/\partial Z$, which is traceless (i.e. in which the $D_g^{(0)}$ component is zero) the induced ensemble average is a weighted combination of Types 2 and 3, giving the computer simulated result [16–18] described in eq. (1).

2.2. *The molecule fixed frame* (x, y, z)

The D symmetry of any quantity in the laboratory frame (X, Y, Z) may be expressed in the molecule fixed frame (x, y, z) by mapping irreducible representations [26, 27] from the $R_h(3)$ point group on to the molecular point group. Table I gives a selection of symmetry mappings on to thirty six of the molecular point groups, ranging from lowest symmetry (C_1) to the high symmetry molecular point groups such as O_h. The significance of such mappings has been described by Whiffen [9] and is summarised in Principle 2.

Table I describes the symmetry of a scalar, pseudo-scalar, polar and axial vector, and the product $\boldsymbol{AA}$ of two vectors in each molecular point group. The latter may be a product either of two polar or of two axial vectors, and includes the scalar, vector and tensor components as described in the heading to column six of the table. Column 2 of the table gives the t.s.r. of each point group, and the other columns record the number of times the t.s.r. occurs in the quantity being described in each column. Using Principle 2 we can see, for example, that the existence or otherwise of ensemble averages in frame (x, y, z) of each point group is also determined[9] by the number of occurrences of the t.s.r.

Taking the C_{2v} point group of water as an example the table, used with Principle 2, shows that the ensemble average $\langle \dot{\boldsymbol{v}}\rangle_{(x,y,z)}$ may exist in frame (x, y, z) because the molecular linear acceleration is a polar vector whose symmetry representation in the point group C_{2v} is given in column 5. This includes the t.s.r. once, and by Principle 2, one scalar component of the ensemble average of linear acceleration may exist in frame (x, y, z). To find which component, we refer to the character table [26, 27] for C_{2v}, and find that A_1 refers to the z axis. We conclude that the ensemble average $\langle \dot{v}_z\rangle$ may exist by Principle 2 in frame (x, y, z). This finding is overlooked by conventional diffusion theory, and it is important to note that the same average vanishes in frame (X, Y, Z) by Principle 1. For a complete picture of statistical processes we need both frames of reference. This can be achieved with combined and systematic use of computer simulation and g.t.s.m.

In other molecular symmetries more than one scalar component of this type may exist in frame (x, y, z), depending on the number of occurrences of the t.s.r. In the chiral group C_1 for example there are three occurrences of the t.s.r. both for axial and polar vectors (columns 4 and 5 respectively) and this means that the x, y, and z scalar ensemble averages over both types of vector may exist in frame (x, y, z). In each case average is independent, and each has a different magnitude. By Principle 1 they all vanish, however, in frame (X, Y, Z). In a high symmetry point group such as T_d, for example that of methane, there are no occurrences of the t.s.r. in columns 4 and 5, and in consequence there can be no surviving scalar components of ensemble averages over vector quantities in frame (x, y, z). In C_{4h} the point group's t.s.r. appears once in column four, but not in column five, signifying one

component ensemble average over an axial vector such as the angular acceleration in frame (x, y, z). Note that in the chiral point groups C_n and D_n there are always occurrences of the t.s.r. in both columns 4 and 5.

The number of occurrences of the t.s.r. of column 2 in column 6 signifies the number of independent scalar elements that may exist in frame (x, y, z) of the ensemble average $\langle AA \rangle_{(x,y,z)}$. In the molecular point group of lowest symmetry, C_1, nine scalar components of this ensemble average may exist in frame (x, y, z). For the correlation function $\langle A(t)A(0) \rangle_{(x,y,z)}$ each may have a different time dependence, even at field free equilibrium. In frame (X, Y, Z) in contrast, Principle 1 implies that only the auto correlation function may exist, with one independent time dependence. There is only one occurrence of the t.s.r. in frame (X, Y, Z), but no less than nine in frame (x, y, z) for the same diffusion process. These are the three diagonal and six off diagonal elements, all with different time dependencies. All may change sign from one enantiomorph to the other.

In point groups of higher symmetry, such as C_{2v}, there are fewer occurrences of the t.s.r. in column six, indicating the existence of fewer independent elements of the ensemble average. In C_{2v} there are three occurrences of the group's t.s.r. in column 6, and a little group theory is needed to interpret their meaning. The result in column 6 for this point group, as for all point groups, is obtained using products of irreducible representations for two polar vectors, for example, is

$$(A_1 + B_1 + B_2)(A_1 + B_1 + B_2) = A_1A_1 + A_1B_1 + A_1B_2 + B_1A_1 + B_1B_1 + B_1B_2 + B_2A_1 + B_2B_1 + B_2B_2 \quad (11)$$

from which

$$A_1A_1 = A_1; \quad B_1B_1 = A_1; \quad B_2B_2 = A_1 \quad (12)$$

using the rules [26, 27] for products of irreducible representations. The character table for C_{2v} finally shows that the products in eq. (12) represent the three ensemble averages

$$\langle A_x(t)A_x(0) \rangle; \quad \langle A_y(t)A_y(0) \rangle; \quad \langle A_z(t)A_z(0) \rangle \quad (13)$$

each with a different time dependence in frame (x, y, z). This is verified precisely by computer simulation [1–5]. In the laboratory frame there is only one ensemble average, the auto correlation function with the symmetry of the t.s.r. $D_g^{(0)}$.

Similarly we may interpret the significance of the t.s.r. occurrences in the other point groups of Table I as they appear in column 6. In some high symmetry groups such as T_d there is only one occurrence, signifying the one **independent** element

$$\langle A_x(t)A_x(0) \rangle = \langle A_y(t)A_y(0) \rangle = \langle A_z(t)A_z(0) \rangle. \quad (14)$$

In other point groups such as C_{3v} there are two occurrences, signifying

$$\langle A_z(t)A_z(0) \rangle \neq \langle A_y(t)A_y(0) \rangle = \langle A_x(t)A_x(0) \rangle, \quad (15)$$

i.e. two independent elements. In some of the low symmetry point groups off-diagonal elements may also exist in addition.

2.3. *The effect of external fields*

The effect of external fields on averages such as these is to change their individual time dependencies. The overall symmetry, in contrast to frame (X, Y, Z). remains the same, and is given by Table I. It is essential therefore to investigate the overall N particle ensemble dynamics in both frames for a complete understanding of the diffusional process.

At field-on equilibrium in the presence of shear, for example, we have asymmetric averages induced in frame (X, Y, Z) of type (1) which are part of the overall ensemble average $\langle \boldsymbol{vv} \rangle$. The latter's symmetry in frame (x, y, z), however, remains the same, and is given in column six of Table I. For each molecular symmetry, therefore, the signature of shear in frame (x, y, z) is different. In frame (X, Y, Z) its symmetry signature is always the same, and is the sum of D symmetries at the head of column six. We conclude that there is a rich variety of behaviour in molecular liquids subjected to Couette flow. As usual, symmetry patterns should be investigated in both frames of reference.

Similar considerations apply in frame (x, y, z) for molecular liquids under the effect of an electric or magnetic field. The external field changes the time dependencies of the individual ensemble averages in frame (x, y, z) but leaves the symmetry patterns of Table I unchanged. In frame (X, Y, Z), however, the fields induce new ensemble averages according to Principle 3.

3. Two physical examples of the application of G.T.S.M.

In this section we provide two applications of g.t.s.m. in an experimental context. The first is its use to provide an explanation for the Weissenberg effect [13–15] and the second is the theoretical prediction of a new form of depolarised light scattering from sheared atomic and molecular N particle ensembles. In both cases cross correlation functions are observed experimentally.

3.1. *The Weissenberg effect*

The Weissenberg effect is observed experimentally as the flow imparted to a sheared liquid in an axis perpendicular to that of the applied shear plane. It is important in industrial contexts, because the perpendicular flow is caused by a pressure great enough to cause damage, for example to rollers in the print industry.

The first explanation for the effect has been reported fully elsewhere [16], and is due to new cross correlation functions between elements of the pressure tensor (or stress tensor) in a sheared N particle ensemble. These can have asymmetry properties analogous to those in eq. (1) of this paper, as illustrated in Ref. [16], Fig. 11. The existence of these new elements was anticipated by g.t.s.m. and confirmed by n.e.m.d. [16–18]. They are apparently unknown to conventional rheology and were first characterised by computer simulation. Their description in conventional terms probably requires new constitutive equations and phenomenological parameters. However, it is clear that the underlying cross correlation functions can be observed experimentally by using computer simulation to match experimental data on Weissenberg flow.

3.2. *Depolarised light scattering from a sheared ensemble*

In this section we argue for the existence of a hitherto unmeasured component of depolarised light scattered from an N particle ensemble subjected to shear strain. For ensembles of atoms and molecules of symmetry higher than T_d,

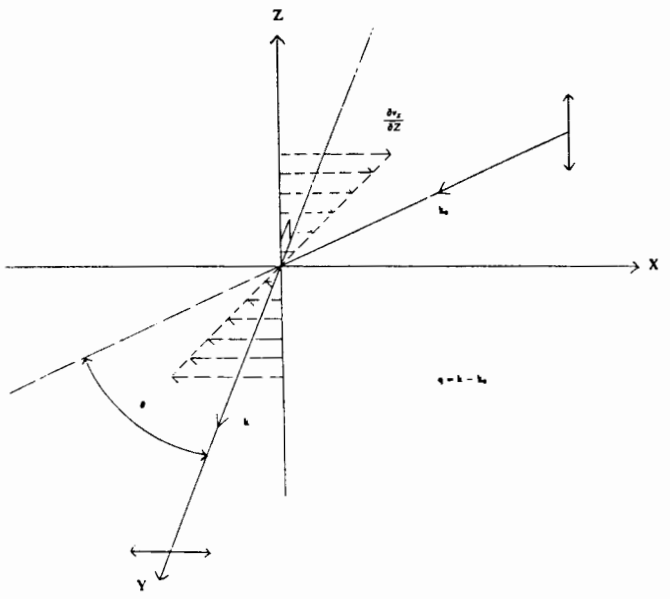

Fig. 1. Light scattering geometry for depolarised light scattering from a sheared N particle ensemble.

where the anisotropy of polarisability vanishes in the absence of collision induced effects [35], this is the only component, and is related by Fourier transform to the new c.c.f. of type (1). The latter is known from computer simulation [16–18] to be directly related to the non-Newtonian nature of the sheared N particle fluid, and in consequence, depolarised light scattering from the sheared fluid is a direct spectral method of probing non-Newtonian dynamics.

The third principle of g.t.s.m. allows the existence of the new current correlation function [36, 37]

$$C_{XZ} = \langle v_X(0)v_Z(t)\exp(i\boldsymbol{q}\cdot(\boldsymbol{r}(0) - \boldsymbol{r}(t)))\rangle \tag{16}$$

in an N particle ensemble subjected to the shear strain $\partial v_X/\partial Z$. This has the same asymmetry properties as type (1). Here $\boldsymbol{q}$ is the scattering vector and

$$\boldsymbol{r}(t) - \boldsymbol{r}(0) = \Delta\boldsymbol{r}(t) = \int_0^t \boldsymbol{v}(t)\,dt, \tag{17}$$

where $\boldsymbol{v}$ is the centre of mass velocity of the diffusing particle (atom or molecule).

We have

$$\langle \Delta r^2(\tau)\rangle = \int_0^\tau \int_0^\tau \langle v_X(t_1)v_Z(t_2)\rangle\,dt_2\,dt_1 \tag{18a}$$

$$= 2\int_0^\tau (t - \tau)\langle v_X(0)v_Z(t)\rangle\,dt. \tag{18b}$$

The current c.c.f. (16) is related to a self dynamic structure factor by

$$F_{XZ}^{(s)}(\boldsymbol{q}, t) = \langle \exp(i\boldsymbol{q}(\boldsymbol{r}(0) - \boldsymbol{r}(t)))\rangle \tag{19}$$

which upon double differentiation provides

$$\frac{d^2}{d\tau^2} F_{XZ}^{(s)}(\boldsymbol{q}, \tau) = -q^2 C_{XZ}(\tau). \tag{20}$$

Equation (20) gives the result

$$J_{XZ}^{(s)}(\boldsymbol{q}, \omega) = \frac{\omega^2}{q^2} S_{XZ}^{(s)}(\boldsymbol{q}, \omega) \tag{21}$$

where J is the temporal Fourier transform of C_{XZ}, and S that of eq. (19). The latter is the intermediate scattering function in the ideal self-dynamic limit for the sheared N particle ensemble. Equation (21) shows that this is related to the new current c.c.f. defined by eq. (16).

3.3. *Light scattering geometry*

Integrating eq. (20) gives the result

$$\lim_{q\to 0}\left(\frac{d}{dt} F_{XZ}^{(s)}(\boldsymbol{q}, t)_{\tau > \tau_l}\right) = -q^2 \int_0^\infty \langle v_X(0)v_Z(t)\rangle\,dt, \tag{22}$$

where τ_l is the correlation time. This shows that the intermediate scattering function S is related to the cross correlation function of Type 1 generated by shear. The function S is observable by light scattering where the initial polarisation vector is in the X axis of the laboratory frame (X, Y, Z) and where the scattered polarisation vector is in the Z axis of this frame. The plane XZ is that of the shear strain $dv_X/\partial Z$.

The existence of shear induced c.c.f.'s of Types 1 and 16 means that there will be depolarised light scattered from a sheared N particle ensemble with intensity S. This spectrum is related to the temporal Fourier transform of eq. (16) by eq. (21).

In atomic ensembles, or in ensembles of molecules of symmetry greater than T_d, this will be the sole contribution to the new type of shear induced light scattering apart from small contributions from collision induced polarisation anisotropies. At equilibrium in the absence of shear, this spectrum will disappear, because the c.c.f.'s of Types 1 and 16 both disappear.

In order to observe the spectrum experimentally, the incident laser beam, polarised in the X axis, is scattered conveniently from an arrangement of co-axial cylinders, and scattered radiation is observed polarised in the axis Z for given scattering angle, angular frequency and scattering vector. This is the spectrum S which gives J by eq. (21), and thus the temporal Fourier transform of eq. (16). The inner cylinder (a stirring rod) rotates rapidly and the outer cylinder is the wall of a round light scattering cuvette. This arrangement creates a shear on a liquid held between the cylinders. The geometry is illustrated in Fig. 1.

The high frequency wing of the spectrum S is amplified by the multiplication by the square of the angular frequency in eq. (21) to give the second spectral moment J. The latter is related directly to the new c.c.f. (16) and this c.c.f. is in turn a direct measure of non-Newtonian effects in a sheared fluid.

The new depolarised spectrum J is therefore a direct measure of the non-Newtonian nature of sheared N particle ensembles.

Depolarised scattering depends solely on the optical anisotropy of the scattering centre, and this may be thought of as a scattering element of polarisability tensor $\boldsymbol{\alpha}$. The scattered electric field vector of the electromagnetic radiation is then

$$E_X = \sum_j \alpha_{XZ}^j \exp(i\boldsymbol{q}\cdot\boldsymbol{r}_j(t)) \tag{23}$$

where α_{XZ}^j is the XZ component of the polarisability tensor $\boldsymbol{\alpha}$ of the jth scattering element, and "q" the scattering vector. Let us situate the centre of mass on an atom of our sheared ensemble. On average, we have, for atomic ensembles

$$\alpha_{XZ}^j = \alpha_0 \frac{\langle R_X R_Z\rangle}{\langle R^2\rangle} \tag{24}$$

where the vector $\boldsymbol{R}$ is defined with respect to the centre of mass of the polarisability element in frame (X, Y, Z), and where the averaged quantity on the r.h.s. of eq. (24) is proportional to the angularly resolved radial distribution function introduced by Heyes and Szczepanski [38]. The latter, denoted by ϱ_{XZ}, is dependent on the positions of nearest neighbours, next nearest neighbours, and so on, around the centre of mass atom, and is assumed here to be approximately the time independent equilibrium average. Therefore we have

$$\alpha^{J}_{XZ} = \alpha_0 \varrho_{XZ}(\boldsymbol{R}) \tag{25}$$

where "$\boldsymbol{R}$" is the argument of the angularly resolved pair radial distribution function. Without loss of generality, we can assume that

$$\varrho_{XZ}(\boldsymbol{R}) = \varrho_{XZ}(\boldsymbol{R}_0) \tag{26}$$

where $\boldsymbol{R}_0$ is the position of the first peak of the pair radial distribution functions. Finally we have

$$\alpha^{J}_{XZ}(t) = \alpha^{J}_{XZ}(0) = \alpha_0 \varrho_{XZ}(\boldsymbol{R}_0) \tag{27}$$

so that the depolarised light scattering spectrum is given by

$$S_{VH}(\boldsymbol{q}, t) \propto \varrho^2_{XZ}(\boldsymbol{R}_0) S^{(s)}_{XZ}(\boldsymbol{q}, t). \tag{28}$$

In order to provide an idea of the frequency and scattering vector dependence of the spectrum J a simulation can be carried out in an ensemble of atoms subjected to shear strain by PUT computer simulation [16–18]. The new current correlation function of Type 16 can be computed directly and its temporal Fourier transform gives J.

3.4. *Polarimetry*

The plane of polarisation of electromagnetic radiation is expected to be changed a little by shearing on the basis of the above argument, and this could be detected with a simple polarimeter, providing a direct method of observing the effect of shear on polarised electromagnetic radiation.

4. New fluctuation–dissipation theorems

The three principles of Section 1 imply the existence of new fluctuation–dissipation theorems, an ideal vehicle for the development of which is the recent theory of Morriss and Evans [31], valid for arbitrary applied field strength. We refer to this as Morriss Evans theory. It is an important step forward in our understanding of n.e.m.d. and provides many new insights to the way in which molecular and atomic ensembles respond to applied force fields of arbitrary strength. The main result of the theory is the relation

$$\langle B(t)\rangle = \langle B(0)\rangle - \frac{F_e}{kT}\int_0^t \langle B(s)J(0)\rangle \, \mathrm{d}s \tag{29}$$

where $B(t)$ is an arbitrary time dependent phase variable of the molecular (or atomic) ensemble, and where F_e and J are respectively the applied force field and dissipative flux, defined by

$$\frac{\mathrm{d}H_0}{\mathrm{d}t} = -JF_e. \tag{30}$$

Here H is the hamiltonian. The integrand on the r.h.s. of eqn. (29) is a **transient time correlation function**, which plays a major role for non-linear, non-equilibrium statistical mechanics analogous to the partion function in thermodynamics and equilibrium statistical mechanics. Equation (29) generalises the Green–Kubo relations [39, 40] and links the non-equilibrium value of a phase variable (the l.h.s.) to the integral over a time correlation function between the dissipative flux $J(0)$ in the equilibrium state and B at a time s after the external field F_e has been turned on. One example of the theorem at work is the relation [39]

$$\eta(t) = -\frac{\langle P_{xy}(t)\rangle}{\dot\gamma} = \frac{V}{kT}\int_0^t \langle P_{xy}(s)P_{xy}(0)\rangle \, \mathrm{d}s \tag{31}$$

for the viscosity, which reduces to the well known Green–Kubo relation in the limit $\dot\gamma \to 0$. Here $\dot\gamma$ is the strain rate and P_{xy} is the off-diagonal component of the pressure tensor. Equation (31) involves a time correlation function between $P_{xy}(0)$ from the equilibrium system and $P_{xy}(s)$ **from the perturbed system**, and is valid for arbitrary strain rate $\dot\gamma$. The Morriss–Evans Theorem thus deals indiscriminately and consistently with linear and non-linear response, thus removing the need for linear response approximation.

4.1. *Application of the theorem to dielectric relaxation and the dynamic Kerr effect*

We consider a static electric force field E_z applied to a dipolar molecular ensemble. It is well known that the field interacts with each molecule through the latter's multipole moments, i.e. the dipole, quadrupole, octopole, and so on. Without loss of generality we can consider that part of the interaction between field and molecular dipole moment. This is characterised by the torue $-\boldsymbol{\mu} \times \boldsymbol{E}$ where $\boldsymbol{\mu}$ is the molecular dipole moment. The energy $\boldsymbol{\mu} \cdot \boldsymbol{E}$ supplements the system hamiltonian. Thus, eq. (29) reads

$$\langle B(t)\rangle = \langle B(0)\rangle - \frac{E_z}{kT}\int_0^t \langle B(s)\dot\mu_z(0)\rangle \, \mathrm{d}s, \tag{32}$$

where $\dot\mu_z$ is the time derivative of μ_z, and is known as the "rotational velocity". Equation (29) thus reads, for example

$$\langle \dot\mu_z(t)\rangle = -\frac{E_z}{kT}\int_0^t \langle \dot\mu_z(s)\dot\mu_z(0)\rangle \, \mathrm{d}s. \tag{33}$$

In Eq. (32), $B(t)$ is in general **any** phase variable of the N molecule ensemble, and this equation allows us to make account of the set of non-vanishing c.c.f.'s induced by E_z of arbitrary strength, $E_z \neq 0$. The following are examples of the new fluctuation–dissipation theorems governing dielectric relaxation and the dynamic Kerr effect.

Setting $B(t)$ to μ_z, we recover a generalisation of the fluctuation dissipation theorem of linear response theory as customarily applied to dielectric relaxation

$$\langle \mu_z(t)\rangle = -\frac{E_z}{kT}\int_0^t \langle \mu_z(t)\dot\mu_z(0)\rangle \, \mathrm{d}s \tag{34}$$

relating the orientational transient $\langle \mu_z(t)\rangle$ to the non-equilibrium time correlation function which is the integrand on the right hand side. Traditional experimental methods use $\mu E_z \ll kt$, but eq. (34) shows clearly that for any applied electric field strength the orientational fall transient is dependent on the field strength. Linear response theory equates the time dependence of the fall transient and the equilibrium orientational autocorrelation function.

The traditional approach also has no method of explaining why time c.c.f.'s such as those of eq. (10) exist for $\boldsymbol{E} \neq \boldsymbol{0}$ and

vanish **if and only if** $\boldsymbol{E} = \boldsymbol{0}$. However, this is easily accommodated by the new Theorem using, for example, $B(t) = \boldsymbol{v}(t)$ or $\boldsymbol{\omega}(t)$, giving the relations

$$\langle \boldsymbol{v}(t) \rangle = -\frac{E_Z}{kT} \int_0^t \langle \boldsymbol{v}(s) \cdot \dot{\boldsymbol{\mu}}(0) \rangle \, \mathrm{d}s \tag{35}$$

and

$$\langle \boldsymbol{\omega}(t) \rangle = -\frac{E_Z}{kT} \int_0^t \langle \boldsymbol{\omega}(s) \cdot \dot{\boldsymbol{\mu}}(0) \rangle \, \mathrm{d}s. \tag{36}$$

The fluctuation–dissipation theorem of type (35) shows the presence of a non-vanishing velocity transient due to the fact that the time c.c.f. $\langle \boldsymbol{v}(t) \cdot \dot{\boldsymbol{\mu}}(0) \rangle$ exists in frame (X, Y, Z), both for $\boldsymbol{E} \neq \boldsymbol{0}$ *and* $\boldsymbol{E} = \boldsymbol{0}$ from the first principle of group theoretical statistical mechanics. The fluctuation dissipation theorem of type (36) shows the existence of a non-vanishing angular velocity transient due to the fact that the time c.c.f. $\langle \boldsymbol{\omega}(t) \cdot \dot{\boldsymbol{\mu}}(0) \rangle$ exists in frame (X, Y, Z) for $\boldsymbol{E} \neq \boldsymbol{0}$ (third principle of group theoretical statistical mechanics) but vanishes in this frame when $\boldsymbol{E} = \boldsymbol{0}$ (first principle). The transient c.c.f.'s exist for $0 < s < t$ in both cases. We can obtain a third expression merely by multipying eqs. (35) and (36), i.e.

$$\langle \boldsymbol{v}(t) \rangle \langle \boldsymbol{\omega}(t) \rangle = \left(\frac{E_Z}{kT} \right)^2 \int_0^t \langle \boldsymbol{v}(s) \cdot \dot{\boldsymbol{\mu}}(0) \rangle \times \mathrm{d}s \int_0^t \langle \boldsymbol{\omega}(s) \cdot \dot{\boldsymbol{\mu}}(0) \rangle \, \mathrm{d}s \tag{37}$$

which involves the product of translational and rotational transients.

4.2. *Experimental observations*

The new fluctuation–dissipation theorems can be investigated by computer simulation for all E_Z, but also provide an opportunity for the experimental observation of transient averages caused by cross correlation functions. An interesting example is $\langle \boldsymbol{v}(t) \rangle$. This vanishes both at field-off thermodynamic equilibrium and field-on equilibrium (the steady state) because of time reversal symmetry. However, it may exist as a transient, and should be observable using conventional apparatus to pulse the molecular ensemble with an applied E_Z. A small net translation should be transiently observable, akin to the well known phenomenon of dielectrophoresis [41] usually attributed to non-uniformities in the applied electric field, i.e. to field gradients. Similarly, eq. (36) shows the existence of a non-vanishing transient angular velocity, which may be observable by techniques sensitive to molecular angular motion, such as far infrar red absorption or nuclear magnetic resonance relaxation. The transient angular velocity is intuitively understandable in terms of a removal of external torque.

5. Computer simulations

To illustrate the results of g.t.s.m. in liquid water the effect of an external Y axis electric field was simulated using methods and conditions described fully elsewhere [42]. The results were as predicted by theory, i.e. the symmetry pattern was changed in frame (X, Y, Z) and remained unchanged in frame (x, y, z). Similar results were obtained for liquid methyl chloride of C_{3v} symmetry for a range of auto and cross correlation functions. There was detailed agreement with g.t.s.m. in both cases. It is expected that further work will pursue the consequencies of shear in a molecular liquid in frames (X, Y, Z) and (x, y, z), and in particular will concentrate on shear induced correlation functions of relevance to depolarised light scattering and the Weissenberg effect.

6. Application to angularly resolved pair radial distribution functions

The radial distribution function has been resolved into angular components by Heyes *et al.* [38] in the context of Couette flow and its computer simulation. This is a probe of atomic and molecular liquid structure which measures the spatial anisotropy of molecules or atoms around any member of the ensemble. It is denoted $g_{\alpha\beta}$ [38, 39] and can be used to probe the rheology of gaseous flow, for example Refs [38]. The subscripts denote Cartesian components of frame (X, Y, Z) and peaks in $g_{\alpha\beta}$ represent the amplitude and position of correlation shells of given symmetry. The radial distribution function can refer to pairs of atoms, denoted i and j, or to multi-particle correlations involving clusters. For pair coordination shells an angular resolution method was found by Heyes and Szczepanski [38] to be critically important in isolating structural changes that the complete r.d.f. tends to obscure. These strong, anisotropic, structural changes are induced by shearing a liquid or gas with a strain rate such as $\partial v_X / \partial Z$ where v_X is an applied velocity component. Angular resolution of the pair r.d.f. showed local shearing strain through computer simulation.

6.1. *The D symmetries of pair and four particle radial distribution functions*

We refer to the angularly resolved accumulator function of Heyes and Szczepanski [38], $f_{\alpha\beta}$. The space around each atom is divided into concentric spherical shells of thickness δr. For each atom in the shell in the range $r \pm \delta r/2$ the function

$$h_{\alpha\beta} = \frac{1}{N} \sum_{i \neq j}^{N} \sum \frac{\langle R_{\alpha ij} R_{\beta ij} \rangle}{\langle R_{ij}^2 \rangle} \tag{38}$$

is accumulated in a computer simulation, usually going out as far as half the molecular dynamics box side. In eq. (38) the accumulator function $f_{\alpha\beta}$ is given with respect to the pair r.d.f., and consequently $R_{\alpha ij}$ is the αth Cartesian component of the vector $\boldsymbol{R}_{ij}$ joining particle i and j. N is the number of atoms over which the number is computed. The angularly resolved r.d.f. is then

$$g_{\alpha\beta}(r) = \frac{V f_{\alpha\beta}(r)}{N V(r)} \tag{39}$$

where $V(r)$ is the volume of the shell bounded by $r \pm \delta r/2$:

$$V(r) = 4\pi r^2 \delta r.$$

The conventional pair r.d.f. leaves out of consideration the Cartesian components and effectively replaces $R_{\alpha ij}$ and $R_{\beta ij}$ in eq. (38) by R_{ij}. The product inside the ensemble average brackets $\langle \, \rangle$, in eq. (38) is a particular scalar element of the tensor product $\langle R_{ij} R_{ij} \rangle$, whose complete D symmetry is

$$D_u^{(1)} D_u^{(1)} = D_g^{(0)} + D_g^{(1)} + D_g^{(2)} \tag{41}$$

In the absence of an applied field, such as shear, only the

ensemble average with the scalar symmetry $D_g^{(0)}$ can have a finite value. This gives the conventional radial distribution function

$$\langle R_{Xij}R_{Xij}\rangle = \langle R_{Yij}R_{Yij}\rangle = \langle R_{Zij}R_{Zij}\rangle = \langle \boldsymbol{R}_{ij}\boldsymbol{R}_{ij}\rangle. \tag{42}$$

We may extend the symmetry arguments to r.d.f.'s at field-off thermodynamic equilibrium involving more than two atoms, i and j. If we consider three atoms, i, j, and k, and denote the vectors connecting them by

$$\boldsymbol{R}_1 \equiv \boldsymbol{R}_{ij}; \quad \boldsymbol{R}_2 \equiv \boldsymbol{R}_{ik}; \quad \boldsymbol{R}_3 \equiv \boldsymbol{R}_{jk}$$

we may in general attempt to construct the angularly resolved triplet r.d.f., whose scalar elements are contained within the triple tensor product $\langle \boldsymbol{R}_1\boldsymbol{R}_2\boldsymbol{R}_3\rangle$ with twenty seven possible components. However, the first principle of g.t.s.m. shows that all of these must vanish at thermodynamic equilibrium from the Clebsch–Gordan expansion

$$\begin{aligned}\Gamma(\boldsymbol{R}_1)\Gamma(\boldsymbol{R}_2)\Gamma(\boldsymbol{R}_3) &= D_u^{(1)}D_u^{(1)}D_u^{(1)} \\ &= D_u^{(0)} + 3D_u^{(1)} + 2D_u^{(2)} + D_u^{(3)}\end{aligned} \tag{43}$$

which does not contain the totally symmetric irreducible representation $D_g^{(0)}$. This type of triplet r.d.f. therefore vanishes at equilibrium. Considering a cluster of four atoms, denoted by i, j, k, and l, there is a possible total of six interconnecting vectors denoted

$$\boldsymbol{R}_1 \equiv \boldsymbol{R}_{ij}; \quad \boldsymbol{R}_2 \equiv \boldsymbol{R}_{ik}; \quad \boldsymbol{R}_3 \equiv \boldsymbol{R}_{il}; \quad \boldsymbol{R}_4 \equiv \boldsymbol{R}_{jl};$$

$$\boldsymbol{R}_5 \equiv \boldsymbol{R}_{kl}; \quad \boldsymbol{R}_6 \equiv \boldsymbol{R}_{jk}.$$

The angularly resolved quadruplet r.d.f. has a total of 729 scalar components contained within $\langle \boldsymbol{R}_1\boldsymbol{R}_2\boldsymbol{R}_3\boldsymbol{R}_4\boldsymbol{R}_5\boldsymbol{R}_6\rangle$. the product of D representations is overall gerade, even to parity inversion

$$\begin{aligned}(D_g^{(1)})^6 &= 15D_g^{(0)} + 36D_g^{(1)} + 40D_g^{(2)} + 29D_g^{(3)} + 15D_g^{(4)} \\ &\quad + 5D_g^{(5)} + D_g^{(6)}\end{aligned} \tag{44}$$

and contains the $D_g^{(0)}$ fifteen times, signifying fifteen independent types of quadruplet angularly resolved r.d.f.'s at equilibrium. These are described in the Appendix as type (1)

$$\langle(\boldsymbol{R}_I \cdot \boldsymbol{R}_J)(\boldsymbol{R}_K \cdot \boldsymbol{R}_L)(\boldsymbol{R}_M \cdot \boldsymbol{R}_N\rangle;$$

$$I = 1, \ldots, 6; \ldots; \quad N = 1, \ldots, 6$$

to type 15

$$\langle(\boldsymbol{R}_I\boldsymbol{R}_J^T) : (\boldsymbol{R}_K\boldsymbol{R}_L^T) \ldots : (\boldsymbol{R}_M\boldsymbol{R}_N^T)\rangle;$$

$$I = 1, \ldots, 6; \ldots; \quad N = 1, \ldots, 6$$

which can be observed in principle in a computer simulation to characterise the angularly resolved equilibrium structure of the atomic liquid in respect of the individual quadruplet clusters it contains. A theory of liquid structure must be capable of reproducing both pair and quadruplet r.d.f.'s self-consistently and match the computer simulations. It is doubtful whether this has been achieved yet, even in atomic liquids.

6.2. *The effect of shear on the pair and quadruplet angularly resolved r.d.f.'s*

Heyes and Szczepanski have verified [38] their existence by effect of shear on gases, liquids, colloids, gels, and suspensions, and have discovered [38, 39] the role of the angularly resolved pair r.d.f. in characterisations of local shear straining. Recently, new time correlation functions between atom velocity components have been simulated by Evans and Heyes [16, 17] using SLLOD and PUT algorithms of non-equilibrium molecular dynamics computer simulation. These results were anticipated with the third principle of g.t.s.m. and do not appear in conventional text book treatments of rheology. It is shown in the appendix how the third principle of g.t.s.m. generates many new angularly resolved cluster and sub-cluster steady state ensemble averages that form the basis of the relevant accumulator and radial distribution functions discovered by Heyes and Szczepanski. Starting our discussion with the simplest of these, described in eqs. (5A) of the Appendix, we have noted there that in the special case $I = J$ Heyes and Szczepanski have verified [38] their existence by SLLOD simulation. For $I = J$ they form the XZ and ZX components of the angularly resolved r.d.f. (2) for an applied strain rate $\partial v_X/\partial Z$.

This is precisely the outcome of principle (3) in this simple case.

The case $I \neq J$ of eq. (5A) of the appendix corresponds to what is termed there a "subcluster" average, in this case a pair sub-cluster of a four atom cluster. Of the six possible ways of linking the four atom cluster we are considering only two, and forming r.d.f.'s based on averages of the type $\langle R_{\alpha ij}R_{\beta kl}\rangle$. These angularly resolved components appear in response to shear.

When considering four out of the six ways of linking a four atom cluster the appendix outlines the many new averages that the shearing field produces. Among these are types (i)–(vi) of the Appendix. Taking Type 1 as an example, we choose as examples $I = 1, J = 2, K = 3, L = 4$. The Type (i) average is therefore $\langle \boldsymbol{R}_{ij} \cdot \boldsymbol{R}_{ik}\boldsymbol{R}_{il} \cdot \boldsymbol{R}_{jl}\rangle$. We are looking at an ensemble average involving the ij, ik, il, and jl pairs of the cluster of four atoms i, j, k, and l. The Type (i) ensemble average written out in terms of scalar components gives accumulator functions for the four vector sub-clusters. For a shear induced by $\partial v_X/\partial Z$ they are (1)

$$f_{XXZX} = \frac{1}{N}\sum_{i\neq j\neq k\neq l}^{N}\sum\sum\sum\left\langle\left\{\frac{R_{Xij}R_{Xik}R_{Zil}R_{Xjl}}{\boldsymbol{R}_{ij} \cdot \boldsymbol{R}_{ik}\boldsymbol{R}_{il} \cdot \boldsymbol{R}_{jl}}\right\}\right\rangle$$

(2)

f_{YYZX}, (3) f_{ZZZX}, (4) f_{XXXZ}, (5) f_{YYXZ}, (6) f_{ZZXZ}.

Each assumulator function provides its own angularly resolved radial distribution function

$$g_{XXZX}(r) = \frac{Vf_{XXZX}(r)}{NV(r)} \tag{45}$$

and so on. The Type (iii) of the Appendix produces the new accumulators : (7) f_{XZXZ}, (8) f_{ZXZX}, (9) f_{ZXXZ}, and (10) f_{XZZX}; providing plenty of scope for the use of computer simulation. All these results are obtained from a simple application of the third principle of g.t.s.m.

6.3. *Non-equilibrium computer simulations*

Non-equilibrium molecular dynamics (n.e.m.d.) computer simulations were performed to test these predictions. PUT shear flow simulations on the Lennard–Jones (LJ) fluid were made at $\varrho = 0.8442$ and $T = 0.722$ using a reduced shear rate of $\dot{\gamma} = 0.0$ and 1.0. The simulations were conducted for

20 000 time steps after equilibration, on 108 LJ molecules. To facilitate the computations, the four particle symmations $f_{\alpha\beta\gamma\delta}$ were made for a restricted set of interactions in which the pair separations were less than 1.1σ. We consider this a valid simplification because the same symmetry rules should apply to a homogeneous subset of four particles as to the total especially as the major source of non-Newtonian behaviour occurs from structural distortions in the short pair separation range. (For the purposes of summation j and k are considered to be neighbours of i, and l is considered to be a neighbour of j.) Taking 100 averages evenely separated over 20,000 time steps ($\Delta t = 0.004$ in reduced units) we found that at $\dot{\gamma} = 0.0$, $f_{XXZX}, f_{YYZX}, f_{ZZZX}, f_{XXXZ}, f_{YYZY}, f_{ZZXZ}, f_{YYYX}$, and f_{YYYZ}, are statistically zero ± 0.002. However, at the moderately shear thinned state of $\dot{\gamma} = 1.0$ ($\eta = 2.04$) $f_{XXZX}, f_{YYZX}, f_{ZZZX}, f_{XXXZ}$, f_{YYXZ}, and f_{ZZXZ} are all statistically non-zero, whereas f_{YYYX} and f_{YYYZ} are statistically zero, in detailed agreement with the third principle of g.t.s.m.

6.4. *The molecule fixed frame (x, y, z), principle 2 of g.t.s.m.*

Principle 2 refers to a molecular rather than an atomic liquid, and in this case allows the evaluation of ensemble averages in frame (x, y, z) of the point group character tables. Radial distribution functions can also be computed for molecular liquids in frame (x, y, z) by mapping the D representations as described earlier in this paper for time correlation functions. Principle 2 then provides the number of non-vanishing averages in the frame (x, y, z) of the point group. Some of the mappings relevant to molecular point groups are summarised in the table of Section 2. A radial distribution function with symmetry $D_g^{(0)} + D_g^{(1)} + D_g^{(2)}$ in frame (X, Y, Z) is equivalent to

$$\Gamma(\langle \boldsymbol{R}_{ij}\boldsymbol{R}_{ij}^T\rangle_{xyz}) = A_1 + (A_2 + B_1 + B_2) + (2A_1 + A_2 + B_1 + B_2) \quad (46)$$

showing three occurrences of the point group's totally symmetric irreducible representation A_1. By Principle 2 there are three possible independent occurrences in frame (x, y, z) providing valuable extra information on the structure of the atomic or molecular liquid using centre of mass or atom pair radial distribution functions.

In the presence of shear, additional $D_g^{(1)}$ and $D_g^{(2)}$ type averages are formed in frame (X, Y, Z). Their equivalents in frame (x, y, z) are independent averages of the Type 9, i.e. the symmetry does not change but the structural details of the pair radial distribution functions reflect the imposed shear. In frame (X, Y, Z), as we have seen, there are extra statistical correlations due to shear. Similar results can be predicted for other sub-cluster averages of interest.

Acknowledgements

The Council of the University of Lancaster and the Academic Board of Royal Holloway and Bedford New College are thanked for the awards of Honorary Research Fellowships to MWE. I.B.M. is thanked for the award of a Visiting Scientist position to MWE and the Academic Board of Royal Holloway and Bedford New College is thanked for the award of an Honorary Lectureship to DMH. The Royal Society of London is thanked for the award of computer time on Cray IS and XMP of the University of London Computer Centre.

Appendix

In this appendix we illustrate the g.t.s.m. rules for isolating the possible non-vanishing angularly resolved radial distribution functions up to order four (the quadruplet), referred to as "cluster averages". We first explain the following basic notations and definitions.

(1) The scalar product of two position vectors $\boldsymbol{R}_I$ and $\boldsymbol{R}_J$ has the symmetry $D_g^{(0)}$.

$$\boldsymbol{R}_I \cdot \boldsymbol{R}_J = R_{IX}R_{JX} + R_{IY}R_{JY} + R_{IZ}R_{JZ}. \quad (1A)$$

(2) The vector product has the symmetry $D_g^{(1)}$

$$\boldsymbol{R}_I \times \boldsymbol{R}_J = \begin{bmatrix} R_{IY}R_{JZ} - R_{IZ}R_{JY} \\ R_{IZ}R_{JX} - R_{IX}R_{JZ} \\ R_{IX}R_{JY} - R_{IY}R_{JX} \end{bmatrix} \quad (2A)$$

(3) The symmetry $D_g^{(2)}$ is the off-diagonal

$$\boldsymbol{R}_I\boldsymbol{R}_J^T = \begin{bmatrix} 0 & R_{IX}R_{JY} & R_{IX}R_{JZ} \\ R_{IY}R_{JX} & 0 & R_{IY}R_{JZ} \\ R_{IZ}R_{JX} & R_{IZ}R_{JY} & 0 \end{bmatrix}. \quad (3A)$$

The sum of the diagonal elements of this matrix is the scalar product $\boldsymbol{R}_I \cdot \boldsymbol{R}_J$. The double dot product $\boldsymbol{R}_I\boldsymbol{R}_J^T : \boldsymbol{R}_K\boldsymbol{R}_L^T$ is the trace of the matrix product. With these definitions it is convenient to develop a systematic shorthand notation with which to examine the possible non-vanishing ensemble averages in angularly resolved pair and quadruplet radial distribution functions.

Field-free equilibrium

(1) The pair or doublet cluster average is generated by eq. (44) of the text. We denote the scalar part of the r.h.s. (i.e. $D_g^{(0)}$) by "0". In field free equilibrium this denotes the one possible type of radial distribution function as described in the text.

(2) The quadruplet cluster average contains no less than fifteen $D_g^{(0)}$ occurrences, denoting by g.t.s.m. fifteen independent types of six vector ensemble averages. To find their different meanings we must examine the generating product of D representations

$$(D_u^{(1)}D_u^{(1)})^3 = (D_g^{(0)} + D_g^{(1)} + D_g^{(2)})^3 \quad (4A)$$

and denoting $D_g^{(1)}$ by "1" and $D_g^{(2)}$ by "2" gives the following 27 possibilities

000 001 002

100 **101** 102

200 201 **202**

010 **011** 012

110 **111** **112**

210 **211** **212**

020 021 **022**

120 **121** **122**

220 **221** **222**

The symbol "000" for example, means a scalar product

$(D_g^{(0)})^3$. Each of thse $D_g^{(0)}$'s have originally come from the dot product part of $D_u^{(1)} D_u^{(1)}$, representing the dot product of two position vectors, e.g. $\boldsymbol{R}_I \cdot \boldsymbol{R}_J$. G.t.s.m. tells us that the ensemble average $\langle \boldsymbol{R}_I \cdot \mathrm{R}_J \rangle$ exists at thermodynamic equilibrium. Thus, what is represented by "000" is a triple dot product average such as $\langle \boldsymbol{R}_I \cdot \boldsymbol{R}_J \boldsymbol{R}_K \cdot \boldsymbol{R}_L \boldsymbol{R}_M \cdot \boldsymbol{R}_N \rangle$. This is one of the fifteen cluster average types represented by the "$15 D_g^{(0)}$" part of eq. (44) of the text. The origin of the other fourteen is made clear by the bolded sets of code numbers in the above section of twenty seven. Each of the bolded code numbers produces $D_g^{(0)}$ in some way. For example **101** represents $D_g^{(1)} D_g^{(0)} D_g^{(1)}$, which corresponds to an allowed ensemble average of the type $\langle \boldsymbol{R}_I \times \boldsymbol{R}_J \cdot \boldsymbol{R}_K \cdot \boldsymbol{R}_L \cdot \boldsymbol{R}_M \times \boldsymbol{R}_N \rangle$. This is the basis upon which the accumulator functions can be built for the angularly resolved radial distribution functions of a cluster of four atoms, interlinked by the six vectors $\boldsymbol{R}_1 \ldots \boldsymbol{R}_6$ as defined in the text. The complete set of fiteeen average types is made up of the following generic members, where I, J, K, L, M, N can each take any value from 1 to 6. This set can be investigated in many interesting ways by computer simulation for $I = 1, \ldots, 6; \ldots; N = 1, \ldots, 6$.

Type 1

$\langle \boldsymbol{R}_I \cdot \boldsymbol{R}_J \boldsymbol{R}_K \cdot \boldsymbol{R}_L \boldsymbol{R}_M \cdot \boldsymbol{R}_N \rangle$

Type 2

$\langle \boldsymbol{R}_I \times \boldsymbol{R}_J \cdot \boldsymbol{R}_K \cdot \boldsymbol{R}_L \cdot \boldsymbol{R}_M \times \boldsymbol{R}_N \rangle$

Type 3

$\langle \boldsymbol{R}_I \boldsymbol{R}_J^T : \boldsymbol{R}_K \boldsymbol{R}_L^T \boldsymbol{R}_M \cdot \boldsymbol{R}_N \rangle$

Type 4

$\langle \boldsymbol{R}_I \cdot \boldsymbol{R}_J \cdot \boldsymbol{R}_K \times \boldsymbol{R}_L \cdot \boldsymbol{R}_M \times \boldsymbol{R}_N \rangle$

Type 5

$\langle \boldsymbol{R}_I \times \boldsymbol{R}_J \cdot \boldsymbol{R}_K \times \boldsymbol{R}_L \cdot \boldsymbol{R}_M \cdot \boldsymbol{R}_N \rangle$

Type 6

$\langle \boldsymbol{R}_I \times \boldsymbol{R}_J \cdot \boldsymbol{R}_K \times \boldsymbol{R}_L \cdot \boldsymbol{R}_M \times \boldsymbol{R}_N \rangle$

Type 7

$\langle \boldsymbol{R}_I \times \boldsymbol{R}_J \cdot \boldsymbol{R}_K \times \boldsymbol{R}_L : \boldsymbol{R}_M \boldsymbol{R}_N^T \rangle$

Type 8

$\langle \boldsymbol{R}_I \times \boldsymbol{R}_J^T : \boldsymbol{R}_K \boldsymbol{R}_L \cdot \boldsymbol{R}_M \times \boldsymbol{R}_N \rangle$

Type 9

$\langle \boldsymbol{R}_I \boldsymbol{R}_J^T : \boldsymbol{R}_K \times \boldsymbol{R}_L : \boldsymbol{R}_M \boldsymbol{R}_N^T \rangle$

Type 10

$\langle \boldsymbol{R}_I \cdot \boldsymbol{R}_J \cdot \boldsymbol{R}_K \boldsymbol{R}_L^T : \boldsymbol{R}_M \boldsymbol{R}_N^T \rangle$

Type 11

$\langle \boldsymbol{R}_I \times \boldsymbol{R}_J : \boldsymbol{R}_K \boldsymbol{R}_L^T : \boldsymbol{R}_M \times \boldsymbol{R}_N \rangle$

Type 12

$\langle \boldsymbol{R}_I \times \boldsymbol{R}_J : \boldsymbol{R}_K \boldsymbol{R}_L^T : \boldsymbol{R}_M \boldsymbol{R}_N^T \rangle$

Type 13

$\langle \boldsymbol{R}_I \boldsymbol{R}_J^T : \boldsymbol{R}_K \boldsymbol{R}_L^T : \boldsymbol{R}_M \cdot \boldsymbol{R}_N \rangle$

Type 14

$\langle \boldsymbol{R}_I \boldsymbol{R}_J^T : \boldsymbol{R}_K \boldsymbol{R}_L^T : \boldsymbol{R}_M \times \boldsymbol{R}_N \rangle$

Type 15

$\langle \boldsymbol{R}_I \boldsymbol{R}_J^T : \boldsymbol{R}_K \boldsymbol{R}_L^T : \boldsymbol{R}_M \boldsymbol{R}_N^T \rangle$

Angular resolution in the fifteen cluster products

These quadruplet cluster ensemble averages intrinsically involve angular resolution with Cartesian components, because the various vector and tensor products may survive ansemble averaging. Only in Type 1 is the product restricted to Cartesian components of the same type. Clearly, Types 1 to 15 contain a vast amount of information about intrinsic structural correlation in an atomic liquid between a given four atom cluster of the complete N atom ensemble.

Sub-clusters

There is no difficulty, in principle, in looking at, for example, a Type 1 or Type 2 cluster r.d.f. with computer simulation, provided enough power is available to obtain good statistics. If not, the quadruplet correlation may be broken down using less than the complete set of six vectors $\boldsymbol{R}_1, \ldots \boldsymbol{R}_6$. Using a subset of any four of these, $\boldsymbol{R}_I, \ldots, \boldsymbol{R}_L$, means that there are available three types of sub-cluster ensemble averages of the following types, for $I = 1, \ldots, 6; \ldots; = 1, \ldots, 6$.

Type 16

$\langle \boldsymbol{R}_I \cdot \boldsymbol{R}_J \boldsymbol{R}_K \cdot \boldsymbol{R}_L \rangle$

Type 17

$\langle \boldsymbol{R}_I \times \boldsymbol{R}_J \cdot \boldsymbol{R}_K \times \boldsymbol{R}_L \rangle$

Type 18

$\langle \boldsymbol{R}_I \boldsymbol{R}_J^T : \boldsymbol{R}_K \boldsymbol{R}_L^T \rangle$

which may be more accessible. Types 16 to 18 provide information about the nature of correlation in a cluster of four atoms using four out of the six possible ways of linking the four atoms with atom to atom position vectors $\boldsymbol{R}$. G.t.s.m. shows that there are three ways of doing this. It also shows that all ensemble averages over products involving odd numbers of position vectors will vanish, and that we cannot use sub-clusters involving five, three, or one linking vectors(s). Considering averages using two out of the six possible vectors gives the nineteenth generic type $\langle \boldsymbol{R}_I \cdot \boldsymbol{R}_J \rangle$. Note that angular resolution is not intrinsic to Types 1, 16 and 19, but is implicitly present in all cluster and sub-cluster averages at field-free equilibrium. We now show that the presence of simple strain rate $\partial v_X / \partial Z$ induces a vast number of possibilities, all of which can be investigated in principle by computer simulation.

Steady state in the presence of shear

The presence of shear with symmetry $D_g^{(0)} + D_g^{(1)} + D_g^{(2)}$ brings into consideration the third principle of g.t.s.m., as explained in the text. The effect on Type 19 generic sub-clusters is to make possible the existence of $D_g^{(1)}$ and $D_g^{(2)}$ ensembles averages represented respectively by $\langle \boldsymbol{R}_I \times \boldsymbol{R}_J \rangle$ and $\langle \boldsymbol{R}_I \boldsymbol{R}_J^T \rangle$. For an applied strain rate involving $\partial v_X / \partial Z$ the extra ensemble averages

$$\langle R_{IZ} R_{JX} - R_{IX} R_{JZ} \rangle \neq 0; \quad \langle R_{IZ} R_{JX} \rangle \neq 0; \langle R_{IX} R_{JZ} \rangle \neq 0 \tag{5A}$$

are expected in the presence of shear at the steady state. For four vector sub-clusters and the full six vector averages of Types 1 to 18 the third principle of g.t.s.m. predicts respectively the appearance of six extra $D_g^{(2)}$ type averages and six

extra $D_g^{(1)}$ type averages (four vector sub-cluster) and for the full six vector cluster no less than forty new types of $D_g^{(2)}$ symmetry and thirty six new types of $D_g^{(1)}$ symmetry. We restrict consideration here to the four vector sub-clusters. The new types of $D_g^{(1)}$ symmetry are, in general, for $I = 1, \ldots, 6$; $\ldots; L = 1, \ldots, 6$

Type (i)

$$\langle (\boldsymbol{R}_I \cdot \boldsymbol{R}_J)(\boldsymbol{R}_K \times \boldsymbol{R}_L) \rangle$$

Type (ii)

$$\langle (\boldsymbol{R}_I \times \boldsymbol{R}_J)(\boldsymbol{R}_K \cdot \boldsymbol{R}_L) \rangle$$

Type (iii)

$$\langle (\boldsymbol{R}_I \times \boldsymbol{R}_J) \times (\boldsymbol{R}_K \times \boldsymbol{R}_L) \rangle$$

Type (iv)

$$\langle (\boldsymbol{R}_I \times \boldsymbol{R}_J)(\times)\boldsymbol{R}_K \boldsymbol{R}_L^T \rangle$$

Type (v)

$$\langle \boldsymbol{R}_I \boldsymbol{R}_J^T (\times)(\boldsymbol{R}_K \times \boldsymbol{R}_L) \rangle$$

Type (vi)

$$\langle \boldsymbol{R}_I \boldsymbol{R}_J^T (\times \times)(\boldsymbol{R}_K \boldsymbol{R}_L^T) \rangle$$

In Types (iv), (v) and (vi) the symbols $(\times)$ and $(\times\times)$ are defined as forming vector products between a conventional three element column vector and the vector part of a three by three tensor. The latter is defined as follows. If $\boldsymbol{R}_I \boldsymbol{R}_J'$, of $D_g^{(2)}$ symmetry, has the form

$$\begin{matrix} \ulcorner\urcorner & \ulcorner\urcorner \\ 0 & a & b \end{matrix}$$
$$\begin{bmatrix} c & 0 & d \\ e & f & 0 \end{bmatrix}$$

then its vector part, of $D_g^{(1)}$ symmetry, is the three element column vector

$$\begin{matrix} \ulcorner\urcorner & \ulcorner\urcorner \\ d & - & f \end{matrix}$$
$$\begin{bmatrix} e - b \\ a - c \end{bmatrix}$$

and the product $\boldsymbol{R}_I \times \boldsymbol{R}_J(\times)\boldsymbol{R}_K \boldsymbol{R}_L^T$ for example is the conventional $\boldsymbol{A} \times \boldsymbol{B}$ where

$$\boldsymbol{A} \equiv \boldsymbol{R}_I \times \boldsymbol{R}_J; \quad \boldsymbol{B} \equiv \begin{matrix} \ulcorner\urcorner & \ulcorner\urcorner \\ d & - & f \end{matrix} \begin{bmatrix} e - b \\ a - c \end{bmatrix}.$$

Similarly we can obtain the six $D_g^{(2)}$ averages giving a total of twelve new sub-cluster averages in response to shear. Each of these contains many angularly resolved components which can be investigated with simulation. Note that type (5A) with $I = J$ have been computed by Heyes and Szczepanski [2], but that the others are unexplored as yet. They are likely to produce a great deal of information about non-Newtonian effects [9–12] such as shear thickening and thinning, the onset of convective and structural turbulence, the formation of two and three dimensional string phases, electrorheology, colloids, and so on. They are incorporated in eqs. (38) and (39) of the text as described for the simple pair r.d.f.

References

1. Ryckaert, J. P., Bellemans, A. and Ciccotti, G., Mol. Phys. **44**, 979 (1981).
2. Evans, M. W., Lie, G. C. and Clementi, E., J. Chem. Phys. **88**, 5157 (1988).
3. Evans, M. W. and Ferrario, M., Chem. Phys. **72**, 147 (1982).
4. Evans, M. W., Phys. Rev. Lett. **50**, 371 (1983).
5. Evans, M. W. and Evans, G. J., Dynamical Processes in Condensed Matter (Edited by M. W. Evans), Vol. 63 of I. Prigogine and S. A. Rice (eds.), Advances in Chemical Physics. Wiley Interscience, New York, (1985).
6. Evans, M. W., Evans, G. J., Coffey, W. T. and Grigolini, P., Molecular Dynamics. Wiley Interscience, New York (1982).
7. Bordewijk, P. and Bottcher, C. J. F., Theory of Electric Polarisation, Vols. 1 and 2. Elsevier, Amsterdam (1973, 1979).
8. Hill, N. E., Vaughan, W. E., Price, A. H. and Davies, M., Dielectric Properties and Molecular Behaviour. van Nostrand/Rheinoldt (1969).
9. Whiffen, D. H., Mol. Phys. **63**, 1053 (1988).
10. Evans, M. W., Chem. Phys. **127**, 413 (1988).
11. Evans, M. W., Chem. Phys. **135**, 187 (1989).
12. Evans, M. W., Phys. Rev. A, Brief, Rep. **39**, 6041 (1989).
13. Harris, J., Rheology and Non-Newtonian Flow. Lognman, London (1977).
14. Schowalter, W. R., Mechanics of Non-Newtonian Fluids. Pergamon, Oxford (1978)..
15. Evans, D. J., Phys. Rev. **A36**, 4514 (1987).
16. Evans, M. W. and Heyes, D. M., Mol. Phys. **65**, 1441 (1988).
17. Evans, M. W. and Heyes, D. M., Phys. Rev. B (in press).
18. Evans, M. W. and Heyes, D. M., Mol. Sim. (in press).
19. Evans, M. W., Phys. Lett. **A134**, 409 (1989).
20. Evans, D. J. and Morriss, G. P., Computer Phys. Rep. **1**, 297 (1984).
21. Heyes, D. M., Mol. PHys. **57**, 1265 (1986).
22. Evans, D. J. and Morriss, G. P., Mol. Phys. **61**, 1551 (1987).
23. Heyes, D. M., Morriss, G. P. and Evans, D. J., J. Chem. Phys. **83**, 4760 (1985).
24. MacGowan, D. and Heyes, D. M., Mol. Sim. **1**, 277 (1988).
25. Hammonds, K. D. and Heyes, D. M., J. Chem. Soc., Faraday Trans. II **84**, 705 (1988).
26. Urch, D. S., Orbitals and Symmetry. Penguin, Harmondsworth (1970).
27. Cotton, F. A., Chemical Applications of Group Theory. Interscience, New York (1964).
28. Evans, M. W., Physica, **131B&C**, 273 (1985).
29. Evans, M. W., Phys. Rev. **A31**, 3947 (1985).
30. Evans, M. W., Phys. Scripta **30**, 94 (1984).
31. Morriss, G. P. and Evans, D. J., Phys. Rev. **A35**, 792 (1987).
32. Neumann, F. E., Vorlesungen uber die Theorie Elastizitat der Festen Korper und des Lichtathers. Teubner, Leipzig (1985).
33. Curie, P., J. Phys. (Paris) **3**, 393 (1894).
34. Barron, L. D., Chem. Soc. Rev. **15**, 189 (1986).
35. Rev. [6], Chapter 11.
36. Berne, B. J. and Pecora, R., Dynamic Light Scattering with Reference to Physics, Chemistry and Biology. Wiley Interscience, New York (1976).
37. Pecora, R. (ed.), Dynamic Light Scattering, Applications of Photon Correlation Spectroscopy. Plenum, New York (1985).
38. Heyes, D. M. and Szczepanski, R., J. Chem. Soc., Faraday Trans. II **83**, 319 (1987).
39. Heyes, D. M., Computer Phys. Rep. **8**, 71 (1988).
40. Hansen, J. P. and McDonald, I. R., Theory of Simple Liquids, 2nd edn. Academic, London (1986).
41. Evans, G. J., in Rev. [5].
42. Evans, M. W., and Heyes, D. M., J. Mol. Liq. (in press). (1989).